

Doping Graphitic and Carbon Nanotube Structures with Boron and Nitrogen



O. Stephan; P. M. Ajayan; C. Colliex; Ph. Redlich; J. M. Lambert; P. Bernier; P. Lefin

Science, New Series, Vol. 266, No. 5191 (Dec. 9, 1994), 1683-1685.

Stable URL:

<http://links.jstor.org/sici?sici=0036-8075%2819941209%293%3A266%3A5191%3C1683%3ADGACNS%3E2.0.CO%3B2-1>

Science is currently published by American Association for the Advancement of Science.

Your use of the JSTOR archive indicates your acceptance of JSTOR's Terms and Conditions of Use, available at <http://www.jstor.org/about/terms.html>. JSTOR's Terms and Conditions of Use provides, in part, that unless you have obtained prior permission, you may not download an entire issue of a journal or multiple copies of articles, and you may use content in the JSTOR archive only for your personal, non-commercial use.

Please contact the publisher regarding any further use of this work. Publisher contact information may be obtained at <http://www.jstor.org/journals/aaas.html>.

Each copy of any part of a JSTOR transmission must contain the same copyright notice that appears on the screen or printed page of such transmission.

JSTOR is an independent not-for-profit organization dedicated to creating and preserving a digital archive of scholarly journals. For more information regarding JSTOR, please contact support@jstor.org.

Doping Graphitic and Carbon Nanotube Structures with Boron and Nitrogen

O. Stephan, P. M. Ajayan,* C. Colliex, Ph. Redlich, J. M. Lambert, P. Bernier, P. Lefin

Composite sheets and nanotubes of different morphologies containing carbon, boron, and nitrogen were grown in the electric arc discharge between graphite cathodes and amorphous boron-filled graphite anodes in a nitrogen atmosphere. Concentration profiles derived from electron energy-loss line spectra show that boron and nitrogen are correlated in a one-to-one ratio; core energy-loss fine structures reveal small differences compared to pure hexagonal boron nitride. Boron and carbon are anticorrelated, suggesting the substitution of boron and nitrogen into the carbon network. Results indicate that single-phase $C_yB_xN_x$ as well as separated domains (nanosize) of boron nitride in carbon networks may exist.

The Kraschmer-Huffman electric arc-discharge process (1) has become a versatile tool to produce carbon nanostructures such as fullerenes (1) and nanotubes (2). Modified versions of this method have been used to create filled C nanotube and nanoparticle composites encapsulating metals (3) and metal carbides (4). Graphite and graphitic fibers have also been modified by intercalation to change the electronic structure and hence the properties (5). Apart from forming intercalated structures and encapsulated nanostructures, a third possibility for modifying graphitic structures exists; this consists in substitutionally replacing the C atoms in the hexagonal network by other elements such as B and N or by isoelectronic compounds that form π -bonded planar layered configurations like graphite. One good example of the latter is hexagonal boron nitride (h-BN), which has an sp^2 hexagonal graphite-like structure.

Hybrids of C, B, and N with a graphite-like structure (CBN sheets) have been synthesized by chemical vapor deposition (CVD) methods from precursor compounds containing the three-component elements (6), and h-BN has been shown to form poorly crystallized turbostratic (rotationally disordered) tubular forms with micrometer diameters as a result of low-temperature chemical decomposition (7). The advantage of the arc-discharge method, however, is that it would produce highly crystalline nanostructures with very little disorder (due to the extremely high temperatures that exist in the C plasma). Recently, the doping of B, N, and h-BN into graphitic nanotubes has been the-

oretically discussed (8). The doping of the C_{60} molecule with B has been experimentally accomplished (9). It has been predicted that the doping of h-BN into graphitic structures (10) would alter the electronic properties because BN has a relatively large band gap compared to graphite, which is a semimetal with a vanishing band gap.

We report here the formation of compos-

ite CBN graphitic sheets, nanotubes, and filaments in a modified electric arc-discharge process for various concentrations of B and N. Transmission electron microscopy (TEM) and electron energy-loss spectroscopy (EELS) were used to evaluate the results. A mixture of elemental B (amorphous; brown powder) and graphite powder (in 1:2 weight ratio) was placed inside a central hole in the graphite anode, and the electric arc discharge was performed between the composite anode and a pure graphite cathode in a nitrogen atmosphere (~ 200 mbar) at 25 V and 100 A, respectively. The inside of the deposit formed on the cathode surface after a few minutes of discharge was broken open, crushed and dispersed in ethanol, and observed in a transmission electron microscope (TOPCON 002B; 200 keV) and a scanning transmission electron microscope (VG HB 501; 100 keV).

The resulting samples contained thin graphitic sheets (~ 5 to 100 nm thick) and tubes and filaments with high aspect ratios (Fig. 1). Closed nanotubes (with no B and N), similar to those formed during arc discharges with pure graphite electrodes, were observed in low densities. Well-graphitized thicker tubes in the size range from 100 nm

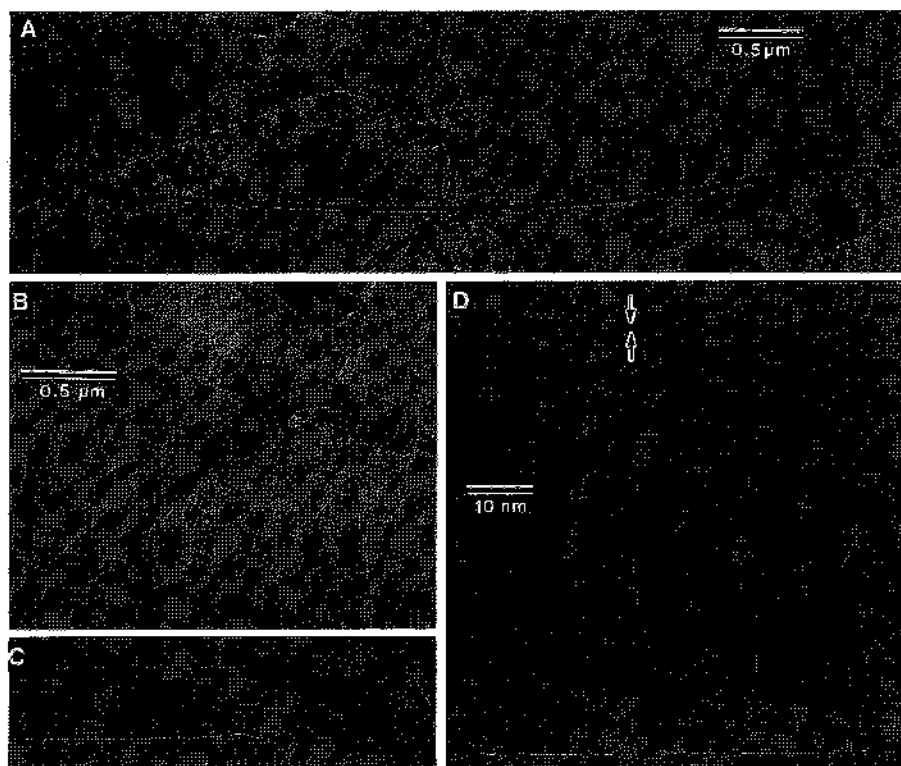


Fig. 1. A series of TEM images showing the morphology of structures described in the text. **(A)** Very long tube running across the micrograph; some sheets (hollow arrows) and pure carbon nanotubes (solid arrow) are shown. **(B)** Thicker, larger graphitic fibers thickened nonuniformly along their lengths. **(C)** Tip of a smaller tube that has not been properly closed; some inside terminations are visible. **(D)** High-resolution image of a large tube showing parallel (002) planes; often groups of planes separated by larger spacing (shown by arrows) are observed on one side of the hollow (regular spacing on other side). However, in some cases, tilting of the sample causes the disappearance of this anomalous spacing, indicating that the larger spacing seen in some images is caused by the orientation of the corners of tubes with polygonal facets (12).

O. Stephan, P. M. Ajayan, C. Colliex, Ph. Redlich, Laboratoire de Physique des Solides, URA 002, Université Paris-sud, Bâtiment 510, 91405 Orsay, France.

J. M. Lambert, P. Bernier, P. Lefin, Groupe de Dynamique des Phases Condensées, URA 233, Université Montpellier II Sciences et Techniques du Languedoc, 34095 Montpellier, France.

*To whom correspondence should be addressed.

to 0.5 μm (Fig. 1B) were seen with tube ends that were ill-formed and not closed (Fig. 1C). Long thin tubes often emerged from thick segments, which suggests that the thickening process was highly nonuniform. The thicker tubular structures contained low concentrations of B and N (typically <2% but sometimes no doping). Thin tubes (50 to

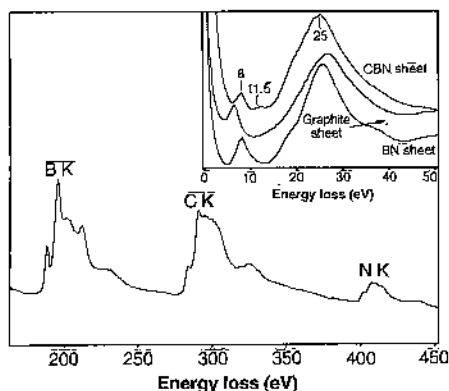


Fig. 2. Core EELS spectra showing the K-shell excitations ($1s-\pi^*$ and $1s-\sigma^*$ regions) of B, C, and N taken from a typical CBN sheet. The spectrum for doped tubes looks the same. (Inset) Low-loss spectra (plasmon) of the same material compared to the spectra from pure graphite and BN. An extra peak is present for the composite material at ~ 11.5 eV.

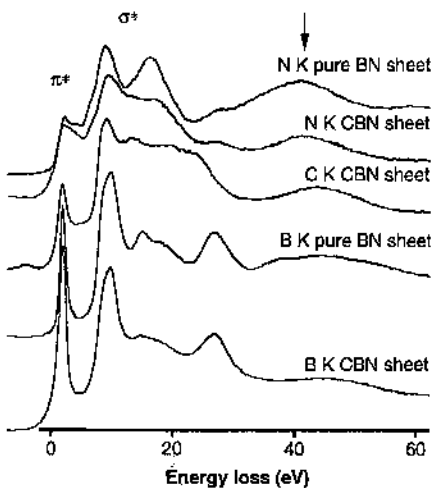


Fig. 3. Fine structures in the core electron K-shell EELS spectra (0.1-eV energy loss per channel) of CBN material compared with that from pure BN for N and B. The approximate composition of the area from which the data were taken corresponds to C_2BN . The intensity levels of the different spectra are scaled for the sake of clear presentation. The y-axis units are arbitrary and not the same for different spectra. The carbon spectrum is given only for the CBN sheet because it is almost identical to that obtained for a pure graphite sheet. The position of the Fermi level is indicated as the zero energy of the spectra. The arrow indicates the position of the peaks that are related to the backscattering from first nearest neighbors in the lattice.

100 nm) of submacroscopic lengths (tenths of millimeters) were often observed (Fig. 1A); the tips of these tubes were rarely seen closed. The very large lengths of such tubes may be correlated with the poorly formed tips or with the inefficiency of forming pentagonal defects (in the presence of B in a nitrogen atmosphere), which are responsible for the closure of the graphitic networks. Concentrations of B and N in such filaments and thin sheets were sometimes quite high (as much as 50%) but generally varied from 0 to 10%. We also found glassy C and polyhedral nanoparticles in the samples. When the electric arc discharge was carried out with h-BN in the anode and in an inert gas atmosphere, no doping was observed.

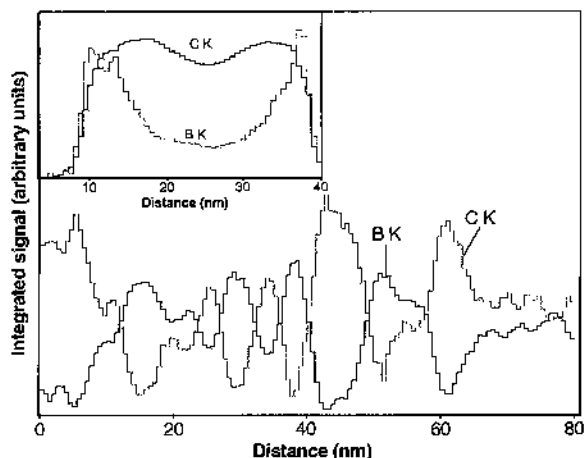
The (002) planes, which characterize the crystallite size and degree of graphitization, were well parallel over most lengths of the tubular structures (Fig. 1D). Diffraction patterns obtained from the tubes indicated similarities with C nanotubes characterized previously but showed evidence for polygonal faceting and three-dimensional ordering (11). The (001) distances are the same as observed for C nanotubes and graphite, with an interplanar spacing of ~ 0.34 nm. For most sheets single-crystal patterns were observed with spacings close to that in graphite, but in rare cases spots split into doublets (12) could be resolved, showing the possible presence of separated domains (of graphite and h-BN). High-resolution TEM images gave indications of perfect crystallinity and also stacking defects, such as larger spacings between planes (see Fig. 1D), but no intercalation was observed.

The EELS spectra taken from the doped graphitic sheets and nanotube structures showed the simultaneous presence of three elements, C, B, and N (Fig. 2 shows the core-loss K edges and low-loss spectra of C, B, and N). In the plasmon energy-loss region, a peak was seen (Fig. 2 inset) around 8

eV of origin similar to that of the 6.5- and 8-eV π^* type plasmon peaks in pure graphite and h-BN, respectively. A dominant peak was observed at ~ 25 eV, identical to the 27- and 25-eV peaks in pure graphite and h-BN, respectively, due to the $\sigma + \pi$ type plasmons. An additional shoulder in the spectrum of the hybrid structure at ~ 11.5 eV distinguishes it from the pure phases.

Comparison of the fine structures of C, B, and N K edges (from composite material) with the corresponding EELS spectra of pure graphite and h-BN (Fig. 3) shows that the features look similar but are not identical. However, the spectra are comparable to those reported for CBN made by CVD (13). The fine structures in the EELS spectra for the N K edge show differences in comparison to pure BN in the $1s-\sigma^*$ region. The σ^* region shows two strong degenerate peaks for pure BN, whereas for composite CBN the second peak is not well resolved and becomes degenerate. The $1s-\sigma^*$ region in CBN for N resembles the $1s-\sigma^*$ region for C in the same material. This suggests that the N core loss features are hybrid and could indicate the presence of N-CB bonds. The distortions in the bond lengths in the network for N (compared to BN and due to N-C bonds) are also reflected by an observed change (~ 2 eV) in the position of the peak due to first nearest neighbor backscattering (14) (see Fig. 3). An apparent shift (chemical) in the energy at maximum for the π peak could be observed for N (~ 0.8 eV toward higher energy) in CBN compared to BN, but this is too small (it is due to changing peak shape) to be interpreted as a real shift in the binding energies. The fine structures of B (σ^*) also show a small deviation compared to BN, but no shifts in the energies of peaks are evident. For C, no obvious changes compared to graphite were observed. The changes in the fine structures in the $1s-\sigma^*$ region give a strong indication of a composite material

Fig. 4. Variation of intensity as the electron beam scans across the specimen (128 spectra per scan). Intensity is normalized with thickness so that the profiles give the concentration of elements. The inset shows the profile for B and C for a 40-nm tube, and the main figure shows the profile for a thin sheet. The electron beam is incident almost parallel to the *c* axis. Perfect spatial anticorrelation is seen for the sheet and to a large extent for the tube. For tubes, doping is higher for the outer layers. In sheets, small domains of separated BN-rich regions surrounded by graphite could exist because the limiting spatial extent of the anticorrelation is ~ 2 to 3 nm. Windows selected for calculating the profiles are 188 to 225 eV for B and 284 to 325 eV for C. The N intensity follows the B profile.



made of C, B, and N (with C-N and C-B bonds), rather than a mechanical mixture of graphite and BN. Furthermore, among the three elements present, B in the lattice, with three unpaired electrons that form in-plane σ bonds, has the highest density of unoccupied π orbitals. Correspondingly, the π peak observed in the spectra is the strongest for B, weaker for C (four electrons), and weakest for N (five electrons).

We estimated the B and N concentrations present in the hybrid structures from measurements of the characteristic signals after background subtraction. The involved cross sections were calculated with the usual σ -K hydrogenic model (15). We always found that B and N were present in the samples in a 1:1 ratio (for all concentrations), which confirms the substitution of the elements into the C network in the (B_xN_x) stoichiometry. However, in some samples taken from the soot that forms in the outer and colder regions of the chamber, EELS structures corresponding to amorphous B were seen with little trace of N. In some cases we observed the stoichiometry C_2BN , matching the composition obtained for CVD-made CBN, but in the majority of cases the average composition corresponded to $C_yB_xN_x$, where $y \gg x$. However, because the electron beam probes local areas, the possibility exists that local areas (nanometers) with C_2BN stoichiometry are surrounded by pure graphite.

Energy-loss line spectra (3, 16) taken from different structures confirm that BN is not deposited as an impurity on the surfaces. Line scans from tubes show that the profiles of the B and N peaks follow shapes similar to that in multilayer tubes, although the shapes are not smooth as we had reported for pure C tubes (3). This could be because the presence of B and N is not uniform along the length or cross section of the tubes and the substitution is spatially random. However, in tubes the doping is higher in the outer layers (Fig. 4 inset). Concentration profiles of B and N in some tubes resemble an outer carbonated BN coating (few layers) for the inner BN-substituted (small amounts) C tubes. The concentrations of B and N are highest in some of the sheets. The line scans across thin planar CBN sheets clearly show (Fig. 4) that the amounts of B (also N) and C present are spatially very well anticorrelated, confirming doping by substitution. The limiting spatial extent of this anticorrelation is of the order of 2 to 3 nm, and the existence of local domains of pure phases with dimensions of this order is quite probable. However, the anticorrelation in the intensity of the EELS peaks proves clearly that the missing C atoms in graphitic networks are replaced and shared by B and N. The same is observed for the tubes.

Our observations of the growth of B- and

N-substituted graphitic and nanotube structures during the electric arc-discharge process is surprising because it has been shown that CBN phases and a mixture of BN and graphite are unstable when annealed (slowly) to temperatures higher than 2000°C and that they decompose to boron carbide and graphite, releasing nitrogen (12). The temperatures that exist in the region where the deposits are formed during the arc-discharge process is >3500°C. In fact, in the outer regions of the chamber where the temperatures are lower, no doping is observed. One possible explanation for the formation of B- and N-substituted graphite, as discussed by others (12), could be the extremely small time scales involved in the reactions in the C plasma; the formation reaction of CBN could occur at a much faster rate than the decomposition reaction to form the carbide phase and nitrogen. Also, because the reaction is carried out in a nitrogen ambient, the equilibrium reaction rates might be shifted in a way that favors CBN formation at elevated temperatures.

REFERENCES AND NOTES

1. W. Kratschmer, L. D. Lamb, K. Fostiropoulos, D. R. Huffman, *Nature* **347**, 354 (1990).
2. S. Iijima, *ibid.* **354**, 54 (1991); T. W. Ebbesen and P. M. Ajayan, *ibid.* **358**, 220 (1992).
3. P. M. Ajayan *et al.*, *Phys. Rev. Lett.* **72**, 1722 (1993).
4. R. S. Fouff, D. C. Lorentis, B. Chan, R. Malhotra, S. Subramoney, *Science* **259**, 346 (1993); M. Tomita, Y. Saito, T. Hayashi, *Jpn. J. Appl. Phys.* **32**, L280 (1993).
5. M. S. Dresselhaus, G. Dresselhaus, K. Sugihara, I. L. Spain, H. A. Goldberg, in *Graphite Fibers and Filaments*, M. Cardona, Ed. (Springer, Berlin, 1988), pp. 244-286.
6. A. R. Badzian, S. Appenheimer, T. Niernyski, E. Oikusunik, in *Proceedings of the Third International Conference on Chemical Vapor Deposition*, F. A. Glaski, Ed. (American Nuclear Society, Hinsdale, IL, 1972), p. 747-752; R. B. Kaner, J. Kouvetakis, C. E. Warble, M. L. Sattler, N. Bartlett, *Mater. Res. Bull.* **22**, 399 (1987).
7. E. J. M. Hamilton *et al.*, *Science* **260**, 659 (1993).
8. J.-Y. Yi and J. Bernholc, *Phys. Rev. B* **47**, 1708 (1993); A. Rubio, J. L. Corkill, M. L. Cohen, *ibid.* **49**, 5081 (1994); Y. Miyamoto, A. Rubio, M. L. Cohen, S. G. Louie, *ibid.* **50**, 4976 (1994).
9. T. Guo, C. Jin, F. E. Smalley, *J. Phys. Chem.* **95**, 4948 (1991).
10. A. Y. Liu, R. M. Wentzcovitch, M. L. Cohen, *Phys. Rev. B* **39**, 1760 (1989).
11. Thicker tubes often show three-dimensional graphitic regions in the cores and edges, as seen from the splitting of (100) and (101) reflections in diffraction patterns and the presence of $(hk\ell)$ spots. Diffraction from most thin long filaments only shows (001) spots [large values of ℓ , up to 12, are sometimes seen suggesting preferential orientation of the (002) planes along the cross section of tubes or flattened tubes] and $(hk0)$ rings suggesting tubular morphology (2). Diffraction also shows the superposition of deformed ellipses for $(hk0)$ rings, which have been shown to arise from tubes with polygonal facets [M. Liu and J. M. Cowley, *Ultramicroscopy* **53**, 339 (1994)]. The $(hk0)$ rings from the tubes extend in the reciprocal space radially, suggesting possible variations in the in-plane spacing, which could depend on the composition of the network (12); but elongation of spots is also indicative of the fibrous structure.
12. A. W. Moore *et al.*, *J. Appl. Phys.* **65**, 5109 (1989); F. Saugnac, F. Teyssandier, A. Marchand, *J. Am. Ceram. Soc.* **75**, 161 (1992).
13. J. Kouvetakis, *et al.*, *Synth. Metals* **34**, 1 (1989).
14. H. Kurata, E. Lefevre, C. Colliex, R. Brydson, *Phys. Rev. B* **47**, 13763 (1993).
15. R. F. Egerton, *EELS in the Electron Microscope* (Plenum, New York, 1986).
16. C. Colliex, *et al.*, *Mikrochim. Acta* **114-115**, 71 (1994).

16 August 1994; accepted 5 October 1994

The Stereochemical Course of Group II Intron Self-Splicing

Richard A. Padgett,* Mircea Podar, Scott C. Boulanger, Philip S. Perlman

The stereochemical specificities and reaction courses for both self-splicing steps of a group II intron have been determined by phosphorothioate substitution at the 5' and 3' splice site phosphodiester bonds. Both steps of the splicing reaction proceeded with a phosphorothioate in the Sp configuration but were blocked by the Rp diastereomer. Both steps also proceeded with inversion of stereochemical configuration around phosphorus, consistent with a concerted transesterification reaction. These results are identical to those found for nuclear precursor mRNA (pre-mRNA) splicing and provide support for the hypothesis that group II introns and nuclear pre-mRNA introns share a common evolutionary history.

Recent work has defined the stereochemical course of nuclear pre-mRNA splicing by means of site-specific substitutions of non-bridging oxygens with sulfur at the splice

junction phosphodiester bonds (1, 2). This substitution produces a chiral center at the phosphorus with two configurations denoted Sp and Rp. The normal oxygen atoms at the prochiral-Rp and prochiral-Sp positions frequently interact differently with enzymes and ribozymes (3). Thus, the analysis of the effects of substitution at these positions can define features of the catalytic site, and anal-

Department of Biochemistry, University of Texas Southwestern Medical Center at Dallas, 5323 Harry Hines Boulevard, Dallas, TX 75235, USA.

*To whom correspondence should be addressed.